International Journal of ISSI, Vol. 13 (2016), No. 1, pp. 1-7

# Mechanical Properties of Dissimilar Welds between AISI 4130 and GOST09ch16N4B

A. H. Madadian [1] , H. Najafi [2]*, M. A. Safarkhanian [3], S. Nategh [4]

[1, 2, 4] *Department of Materials Engineering, Science and Research Branch, Islamic Azad University, Tehran 14515/775, Iran*
[3] *Faculty of Engineering, Majlesi Branch, Islamic Azad University, New Isfahan City, Isfahan, Iran*

## Abstract

Mechanical properties of dissimilar weld joints between GOST09ch16N4B (a martensitic stainless steel) and AISI 4130 thin sheets made by gas tungsten arc welding (GTAW) were studied using ER410NiMo and ER100S-G filler metals in post weld heat treated conditions. Heat treatment cycles consisted of austenitization at 900, 950 and 1000 °C for 1 h and this was followed by oil cooling and tempering at 400 and 500 °C for 1 h. Tensile tests and microhardness measurements were carried out to evaluate the mechanical properties. The base metals, heat affected zones (HAZs) and fusion zones were observed by optical microscope and scanning electron microscope (SEM) equipped with energy dispersive spectroscope (EDS). Based on the results, it was found that the joints strength and microhardness profiles were almost independent of austenitization temperature, but they were affected by the tempering temperature. Increasing the tempering temperature led to the reduction in the hardness of AISI 4130 and the joints strength. Tensile samples were fractured in the base metals. Furthermore, the fracture was shifted from GOST09ch16N4B to AISI 4130 with increasing the tempering temperature. Crack initiation from delta-ferrite led to the fracture in GOST09ch16N4B. Strength and elongation obtained from different PWHTs indicated that tempering at 400 °C resulted in acceptable tensile properties for the weldments made with both filler metals.

*Keywords*: GOST09ch16N4B; AISI 4130; Dissimilar welding; GTAW.

## 1. Introduction

Dissimilar welding has been widely developed in chemical, petrochemical, nuclear power, aerospace and military industries due to the growing demand for design flexibility. Moreover, using dissimilar welding joints with cheaper steels in place of high-alloy steels makes considerable savings in cost. Therefore, numerous dissimilar welding joints between stainless and low alloy steels have received much attention due to the good combination of mechanical properties, formability, weldability and resistance to stress corrosion cracking and other forms of corrosion [1, 2]. Some of the important issues related to the joining of dissimilar steels include: (i) selection of appropriate filler metals, (ii) development of residual stress due to the difference in thermal expansion coefficients of base metals, and (iii) different electrochemical potentials of base metals [3, 4].

Arivazhagan et al. [1] studied the microstructure and the mechanical properties of AISI 304 stainless steel and AISI 4140 low alloy steel joints by gas tungsten arc welding (GTAW), electron beam welding (EBW) and friction welding (FRW). The results showed that the joint made by EBW had the highest tensile strength, as compared with the joint made by GTAW and FRW. It was observed that chromium and nickel were diffused towards AISI 4140 from the AISI 304 and the same happened for iron from AISI 4140 side towards AISI 304.

Hajiania et al. [5] studied dissimilar weldments between AISI 347 austenitic stainless steel and ASTM A335 low alloy steel made by GTAW using ERNICr-3 and ER309L filler metals. A completely austenitic and equiaxed dendritic solidification microstructure containing the precipitates of complex carbides was observed for ERNICr-3 weld metal. They also reported niobium segregation in the inter-dendritic regions. The 309L weld metal solidification microstructure consisted of the skeletal δ-ferrite and the austenitic matrix.

The amount of cold rolling reduction in each stage

* *Corresponding author*
*Tell: +98 21 448 68 481, Fax: +98 21 448 68474*
*Email: hnajafi@srbiau.ac.ir*
*Address: Department of Materials Engineering, Tehran Science and Research Branch, Islamic Azad University, Tehran, Iran. P.O. Box: 14515/775*
*1. M.Sc.*
*2. Assistant Professor*
*3. Assistant Professor*
*4. Professor*

was 72%. So the final thickness of the samples after this procedure was 0.5 mm. Finally, all samples were fully annealed for 3 min at 900 °C. In Fig. 1, A and B denote unidirectional rolling and cross rolling, respectively.

The first number after A/B shows the stage of the samples and the second one represents intermediate annealing. For example, A21 shows the sample after two stage unidirectional cold rolling (before final annealing) with intermediate annealing and A31 is the same one after final annealing.

Because of their acceptable corrosion resistance, good mechanical properties and economy, martensitic stainless steels have become increasingly attractive to a number of industries. GOST09ch16N4B is a Russian standard martensitic stainless steel. $M_{23}C_6$ carbides along with ferrite grains play an important role in determining the mechanical properties of this steel. Based on GOST standard, two heat treatment cycles applied to GOST09ch16N4B include: (i) austenitization at 1140-1160 °C for 5-5.5 h followed by air cooling and tempering at 600-620 °C for 1 h, and (ii) austenitization at 1030-1050 °C for 1 h followed by oil cooling and tempering at 600-620 °C for 1 h [6]. Ebrahimi et al. [7] have reported that carbides are dissolved completely at the austenitizing temperature of 1000 °C for 1 h.

Since the chemical composition of GOST09chl6N4B is not similar to any commonly used AISI 4xx martensitic stainless steels, there are no published studies on similar and dissimilar welding of this kind of martensitic stainless steel. Hence, the objective of this study was to investigate the mechanical properties and the microstructure of dissimilar weldments between GOST09ch16N4B and AISI 4130 thin sheets made by GTAW, using ER100S-G and ER410NiMo filler metals in different post weld heat treated conditions.

## 2. Experimental Methods

The base metals (GOST09ch16N4B and AISI 4130) were supplied in the form of sheets with the thickness of 2.5 mm. Fig. 1 shows the microstructures of base metals consisting of the tempered martensite. Moreover, the δ-ferrite grains elongated in the direction of rolling could be observed in the microstructure of GOST09ch16N4B (Fig. 1b).

The tensile properties of base metals are given in Table 1.

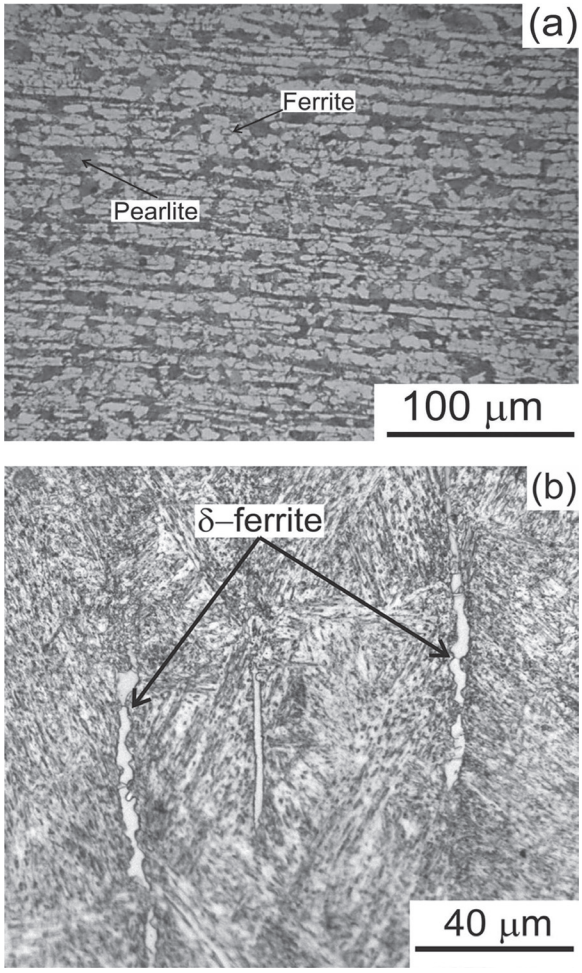


*Fig. 1. Microstructure of as-received base metals: (a) AISI 4130 and (b) GOST09ch16N4B.*

Filler metals were chosen based on their compatibility with one of the base metals. ER100S-G is widely used for the welding of AISI 4130 and ER410NiMo is recommended for the welding of martensitic stainless steels with similar chemical composition. Therefore, ER410NiMo and ER100S-G filler metals were selected to join these metals. The chemical compositions of the base and filler metals are given in Table 2.

In order to prevent cold cracking after welding, both steels were annealed. Annealing included heating at 850 °C for1h (AISI 4130), and 630 °C for 6h (GOST09ch16N4B), which was then followed by furnace cooling.

After that, plates were cut into 150×100×1.5 $mm^3$ coupons with a 60° groove angle for a single-V

Table 1. Tensile properties of the base metals.

| Base Metal | Yield Strength (MPa) | UTS (MPa) | Total Elongation (%) |
|---|---|---|---|
| GOST09ch16N4B | 1030 | 1074 | 16 |
| AISI 4130 | 980 | 1040 | 18 |

Table 2. Chemical composition of base and filler metals (wt. %).

| | C | Mn | Si | Cr | Ni | Mo | Nb | Cu |
|---|---|---|---|---|---|---|---|---|
| GOST09ch16N4B | 0.14 | 0.47 | 0.13 | 16.04 | 0.11 | 0.37 | 0.08 | 0.1 |
| AISI 4130 | 0.3 | 0.28 | 0.15 | 1.05 | 0.19 | 0.66 | - | 0.01 |
| ER410NiMo | 0.01 | - | 0.33 | 11.8 | 4.5 | 0.55 | - | 0.3 |
| ER100S-G | 0.1 | 1.4 | 0.7 | 0.6 | 0.6 | 0.2 | - | - |

groove butt joint configuration. The root face was 0.5 mm with the root opening of 2 mm. The coupons were preheated at 200 °C and then welded along the rolling direction by a single-pass manual GTAW with direct current electrode negative (DCEN) polarity. Argon gas of 99.9% purity level was used as a shielding gas with the flow rate of 15 lit/min. The following welding parameters were optimized based on preliminary experiments and employed for obtaining the final welds for this investigation: current: 116 A, voltage: 12-14 V, welding speed: 2-2.5 mm.s$^{-1}$, and tungsten electrode diameter: 3.2 mm.

Three austenitization temperatures elected for post weld heat treatment (PWHT) included 900, 950 and 1000 °C. After austenitization for 1 h, samples were oil quenched and tempered for 1 h. Tempering temperatures were 400 and 500 °C. For the sake of convenience, the samples are specified in the following section according to the designation given in Table 3.

For microstructural studies, after the conventional metallographic sample preparation, Vilella›s reagent and Nital 2% were used for etching. Scanning electron microscopy was conducted using a Zeiss scanning electron microscope (SEM) equipped with energy dispersive spectroscope (EDS).

Transverse tensile test specimens, with the weld metal at the center of specimens, were prepared according to ASTM E8. The tests were carried out by an Instron 5500R testing machine at a cross-head speed of 1 mm/min. The results reported in this paper were the average of three experiments for each condition. Microhardness survey was also performed along the mid-thickness of the joints in a Doramin Vickers microhardness tester under a load of 100 g and a loading dwell time of 20 s. The reported hardness numbers were the average of four measurements.

## 3. Results and Discussion

Full penetration, defect-free joints were produced by ER410NiMo and ER100S-G filler metals. Fig. 2 illustrates the macrostructure of samples welded with ER410NiMo and ER100S-G.

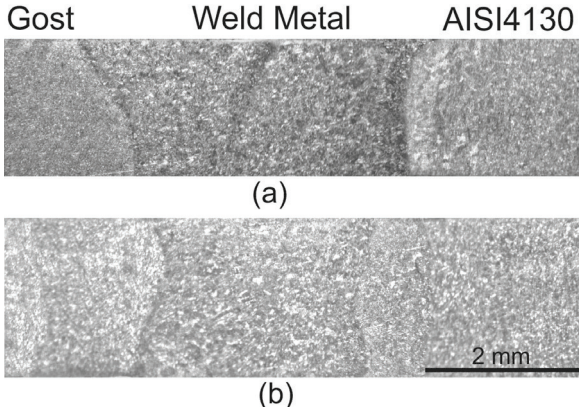


*Fig. 2. Macrostructure of samples welded with: (a) ER100S-G and (b) ER410NiMo filler metals.*

Fig. 3 displays microhardness profiles along the mid-thickness of as-weld specimens. Hardness was

Table 3. Designation of specimens.

| Filler Metal | Austenitization Temperature (°C) | Tempering temperature (°C) | Designation |
|---|---|---|---|
| ER410NiMo | 900 | 400 | M904 |
| | | 500 | M905 |
| | 950 | 400 | M954 |
| | | 500 | M955 |
| | 1000 | 400 | M104 |
| | | 500 | M105 |
| ER100S-G | 900 | 400 | L904 |
| | | 500 | L905 |
| | 950 | 400 | L954 |
| | | 500 | L955 |
| | 1000 | 400 | L104 |
| | | 500 | L105 |

increased from the base metals to the heat affected zone (HAZ), reaching the maximum value of 440 and 460 HV in ER410NiMo and ER100S-G weld metal, respectively. Moreover, the hardness of GOST09ch16N4B (340 HV) was greater than that of AISI 4130 (220 HV).

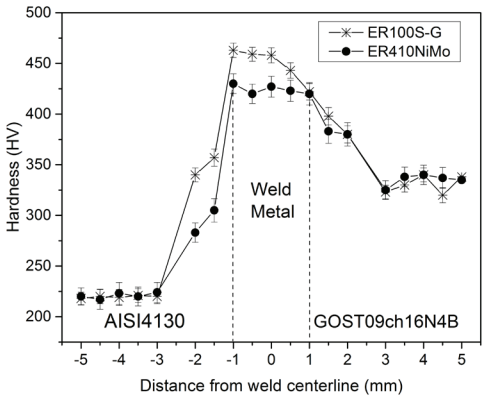


*Fig. 3. Microhardness profile along the mid-thickness of as-weld specimens.*

The presence of martensite colonies in the microstructure of weld metals (Fig. 4) due to their rapid cooling from austenitic region, along with the microsegregation of alloying elements during solidification, which enhanced hardenability, was the main reason for the maximum hardness of weld metals. Optical microscopy of the samples after PWHTs revealed the tempered martensite in the microstructure of both base metals. Fig. 5 shows the microstructures of the base metals after austenitizing at 950 °C and tempering at 500 °C.

Fig. 6 demonstrates microhardness results for the heat treated samples. Increasing the austenitization temperature did not considerably change hardness in different zones, while increasing the tempering temperature from 400 to 500 °C led to decrease in the hardness of AISI 4130 from 430 to 380 HV. However, hardness of GOST09ch16N4B was not influenced by the tempering temperature. It seemed that the presence of strong carbide forming elements such as Nb slowed down the softening of martensite by retarding the recovery of the dislocation substructure. One of the main purposes of adding niobium to the chemical composition of martensitic stainless steels is to enhance the tempering resistance. This is attributed to the secondary hardening reaction and the fine dispersion of MX-type precipitates persisting at high tempering temperatures [8]. Irvine and Picketing [9] also demonstrated the beneficial effects of carbon, nitrogen and niobium on the tempering resistance of 12% Cr steels. As can be seen in Fig. 6, hardness of AISI 4130, unlike GOST09ch16N4B, was considerably reduced in the vicinity of the weld metal. Fig. 7 shows the microstructure of AISI 4130 adjacent to the weld metal after heat treatment.

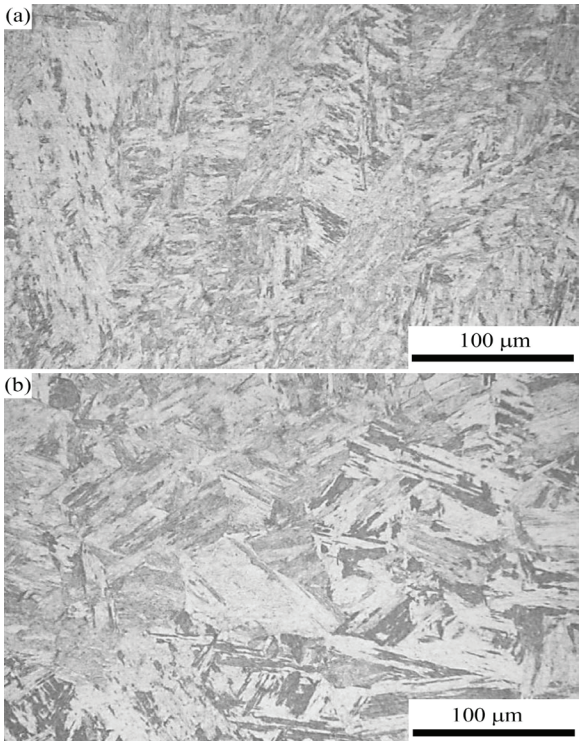


*Fig. 4. Microstructure of: (a) ER100S-G and (b) ER-410NiMo weld metals before heat treatment.*

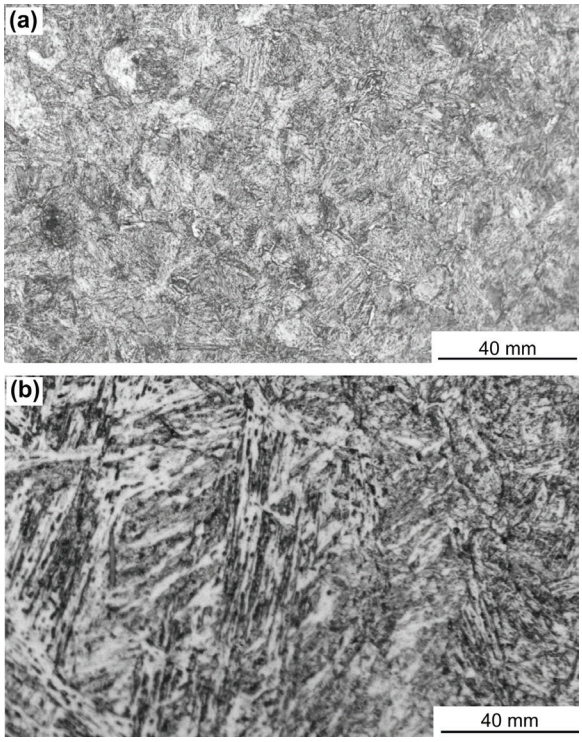


*Fig. 5. Optical microstructure of: (a) AISI 4130 and (b) GOST09ch16N4B after austenitizing at 950* °C *and tempering at 500* °C.

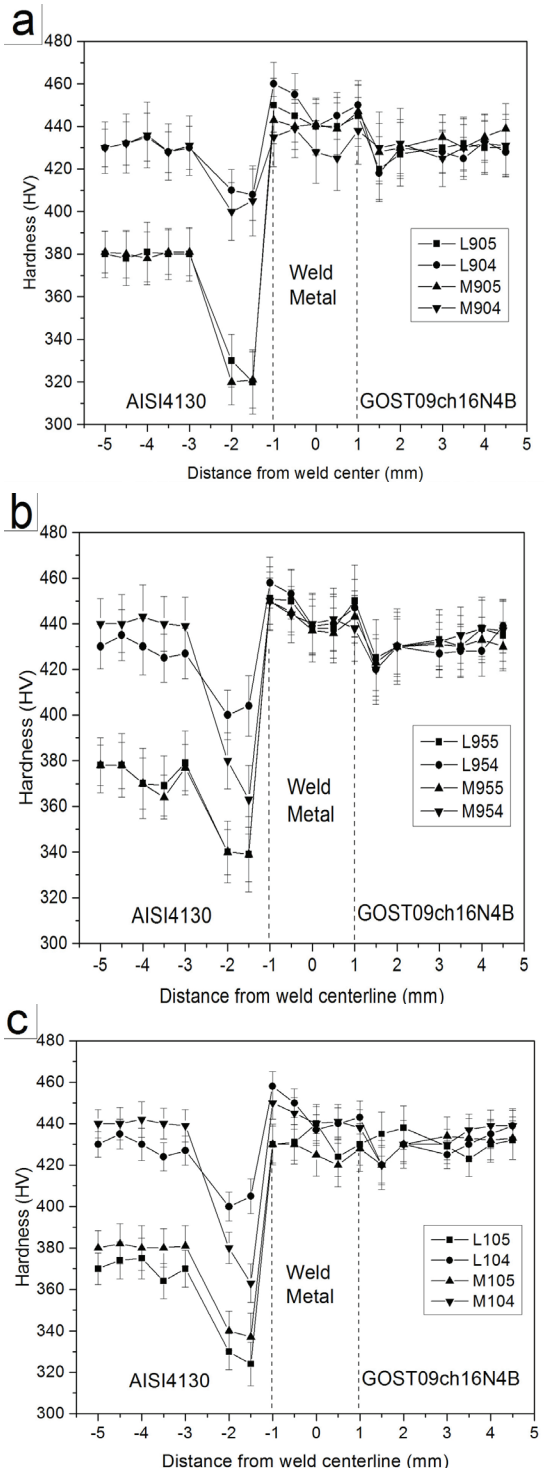


*Fig. 6. Microhardness profiles of heat treated samples austenitized at: (a) 900, (b) 950 and (c) 1000* °C.

In comparison to the base metal (Fig 5(a)), the tempered martensite microstructure consisted of coarser ferritic needles. Moreover, coarse prior austenite grains (approximately greater than 30 μm) were seen in the microstructure of this region. Carbides formed in the microstructure of AISI 4130, i.e., molybdenum and chromium carbides, were readily dissolved at temperatures higher than 700 °C,

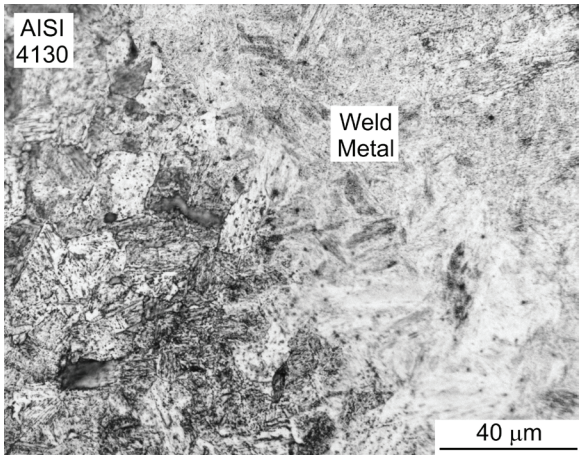


*Fig. 7. Coarse prior austenite grains inherited from AISI 4130 HAZ in a sample austenitized at 950 °C and then tempered at 400 °C.*

leading to austenite grain growth in the HAZ during welding [10]. Therefore, the reduction in hardness could be attributed to the coarse prior austenite grains inherited from AISI 4130 HAZ. On the other hand, several studies conducted on the microalloyed and low alloy steels have demonstrated the effective role of niobium in the retardation of austenite grain growth due to the formation of MX-type carbonitrides [11-14]. Hence, it is expected that the presence of niobium limits austenite grain growth in the HAZ of GOST09ch16N4B. Moreover, since the carbon content of AISI 4130 is higher than that of both ER410NiMo and ER100S-G, the migration of carbon from AISI 4130 to the weld metals may occur during heat treatment, thereby increasing martensite softening [3, 15].

The ultimate tensile strength (UTS) of as-weld samples was approximately 519 MPa with the elongation of 18.2% for both filler metals. The strength was equal to that of annealed AISI 4130 and fractures occurred in AISI 4130 side.

UTS of heat treated samples was influenced by the tempering temperature while it was approximately independent of autenitization temperature (Fig. 8(a)). Increasing the tempering temperature led to the reduction in strength. Furthermore, fracture was shifted from GOST09ch16N4B to AISI 4130 side by increasing the tempering temperature (Fig. 9). It could be concluded from Fig. 6 that fracture occurred in the softer base metal at the tempering temperature of 500 °C. However, at the tempering temperature of 400 °C, the hardness of both base metals was approximately the same and crack initiation from delta-ferrite in the microstructure of GOST09ch16N4B led to the fracture. Fig. 10 shows the microstructure beneath the fracture surface (perpendicular to loading direction) of a tensile sample fractured in GOST09ch16N4B. This figure demonstrates crack propagation from delta-ferrite.

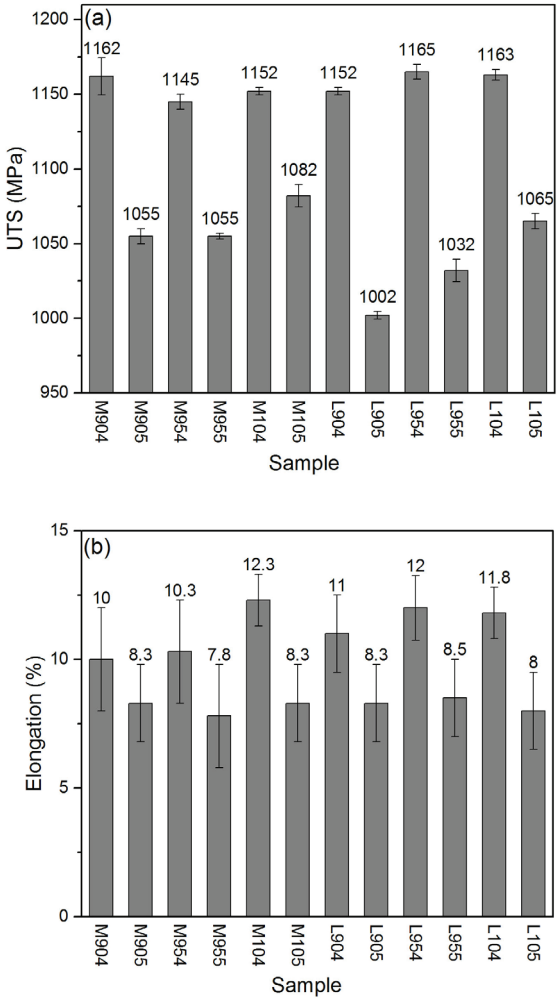


*Fig. 8. Tensile properties of heat treated samples welded with ER100S-G and ER410NiMo: (a) UTS and (b) elongation.*

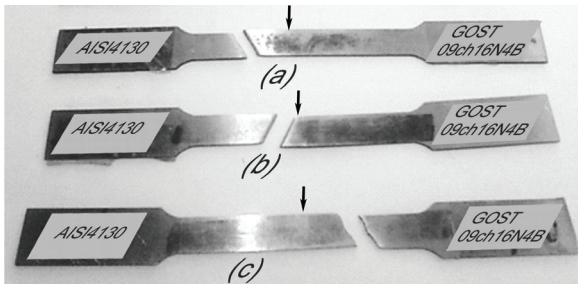


*Fig. 9. Fractured tensile samples (arrows indicate the weld metals): (a) L905, (b) M905 and (c) M904.*

Tensile test of the specimens tempered at 500 °C revealed that failure location in samples welded with ER410NiMo was different from that welded with ER100S-G. The fracture was shifted from HAZ in samples welded with ER410NiMo to the base metal in samples welded with ER100S-G (Fig. 9). Detailed microstructural studies showed coarse carbides were formed adjacent to the weld metal in the microstructure of samples welded with ER410NiMo (Fig. 11), while these precipitates were not observed in the microstructure of samples welded with ER100S-G.

*Fig. 10. Crack propagation along delta-ferrite (indicated by arrow) in the microstructure beneath the fracture surface (perpendicular to the loading direction) of a tensile sample fractured from GOST09ch16N4B side.*

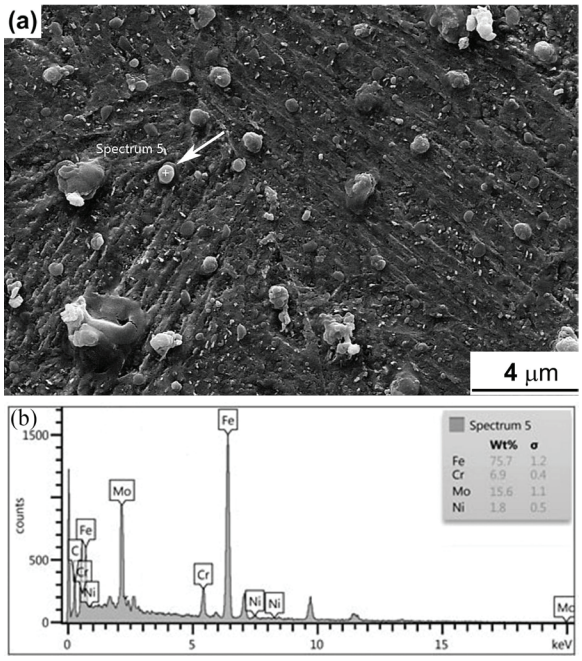


*Fig. 11. (a) Coarse carbides formed in base metal adjacent to the weld metal in the microstructure of samples welded with ER410NiMo, and (b) the results of energy dispersive spectroscopy (EDS) from the precipitate indicated by the arrow.*

This behavior could be related to the greater amount of chromium (a carbide forming element) in the chemical composition of ER410NiMo. Chromium can be diffused from the weld pool to the adjacent base metal where the base metal is partially melted

as a result of high temperature during welding. Fig. 12 shows the EPMA elemental mapping results for the variation of chromium across the fusion boundary (indicated by the dashed line) between AISI 4130 and ER410NiMo. It was observed that chromium concentration was gradually decreased from fusion boundary to AISI 4130 base metal in a distance of about 1 mm. Therefore, chromium carbides formed in the base metal could act as initiation sites for the cracks, thereby leading to fracture.

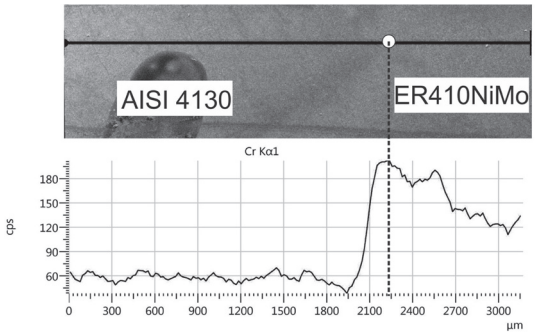


*Fig. 12. Chromium distribution across the fusion line between AISI 4130 and ER410NiMo. The dashed line indicates the fusion boundary between the filler metal and the base metal.*

Elongation of specimens tempered at 400 and 500 °C has been compared in Fig. 8(b). Although the lower tempering temperature resulted in little increase in the elongation, the difference between the maximum and minimum elongations was less than 5%. By considering the strength and elongation combinations in Fig. 8, it could be concluded that tempering at 400 °C led to an acceptable combination of strength and ductility for the weldments obtained by employing ER410NiMo and ER100S-G filler metals.

## 4. Conclusions

- Acceptable dissimilar weld joints between GOST09ch16N4B and AISI 4130 thin sheets were obtained by gas tungsten arc welding using ER410NiMo and ER100S-G filler metals in as-weld and post weld heat treated conditions.
- Joint strength and microhardness profiles were almost independent of austenitization temperature, but they were affected by the tempering temperature. Increasing tempering temperature from 400 to 500 °C led to the reduction in the hardness of AISI 4130 base metal and joint strength.
- Fracture of all tensile specimens occurred in the base metals and it was shifted from GOST09ch16N4B to AISI 4130 by increasing the tempering temperature.
- Based on the observations, crack initiation from delta-ferrite was responsible for fracture in GOST09ch16N4B.
- In samples tempered at 500 °C, the fracture was shifted from HAZ of AISI 4130 to the base metal by changing the filler metal from ER410NiMo to ER100S-G, respectively. It seemed that coarse carbides formed adjacent to the weld metal in the microstructure of samples welded with ER410NiMo acted as crack initiation sites, thereby leading to the fracture.
- Comparing the strength and elongatio combinations obtained from different PWHTs indicated that tempering at 400 °C led to acceptable tensile properties for the weldments made with ER410NiMo and ER100S-G filler metals.

## References

[1] N. Arivazhagan, S. Singh, S. Prakash and GM. Reddy: Mater., Design., 32(2011), 3036.
[2] S.M. Shushan, A.E. Charles and J. Congleton: Corros. Sci., 38(1996), 673.
[3] C.D. Lundin: Weld. J., 61(1982), 58s.
[4] M. Sireesha, V. Shankar, S.K. Albert and S. Sundaresan: Mater. Sci. Eng. A., 292(2000), 74.
[5] I. Hajianniaa, M. Shamanianb and M. Kasiria: J. Adv. Mater. Proc., 1(2013), 33.
[6] GOST 5632-1976 standard.
[7] G.R. Ebrahimi, H. Keshmiri and A. Momeni: Ironmak. Steelmak., 38(2011), 123.
[8] D.T. Llewellyn and R.C. Hudd: Steels: Metallurgy and Applications, 3rd ed., Butterworth-Heinemann, Oxford, (1998).
[9] K.J. Irvine and F.B. Pickering: ISI Special Report., 86(1964), 34.
[10] R.W.K Honeycomb: Steels Microstructures and Properties, Edward Arnold, London, (1980).
[11] A.J. DeArdo: Int. Mater. Rev., 48(2003), 371.
[12] A.B. Cota, C.A.M. Lacerda, F.L.G. Oliveira, F.A. Machado and F.G. da Silva Araujo: Scripta Mater., 51(2004), 721.
[13] S.G. Hong, K.B. Kang and C.G. Park: Scripta Materialia, 46(2002), 163.
[14] M.D.C. Sobral, P.R. Mei and H.J. Kestenbach: Mater. Sci. Eng., A., 367(2004), 317.
[15] C. Pan, R. Wang and J. Gui: J. Mater. Sci., 61(1992), 302.